Lab on a Chip

PAPER

View Article Online
View Journal | View Issue

Cite this: *Lab Chip*, 2018, **18**, 1461

A microfluidic biochip platform for electrical quantification of proteins†

Enrique Valera,[abc] Jacob Berger,[abc] Umer Hassan,[abc] Tanmay Ghonge,[abc] Julia Liu,[ac] Michael Rappleye,‡[abc] Jackson Winter,[ac] Daniel Abboud,[ab] Zeeshan Haidry,[ab] Ryan Healey,[ac] Na-Teng Hung,[ab] Nathaniel Leung,[ab] Naif Mansury,[ac] Alexander Hasnain,[ac] Christine Lannon,[ac] Zachary Price,[ac] Karen White[c] and Rashid Bashir *[abcd]

Received 12th January 2018,
Accepted 6th April 2018

DOI: 10.1039/c8lc00033f

rsc.li/loc

Sepsis, an adverse auto-immune response to an infection often causing life-threatening complications, results in the highest mortality and treatment cost of any illness in US hospitals. Several immune biomarker levels, including Interleukin 6 (IL-6), have shown a high correlation to the onset and progression of sepsis. Currently, no technology diagnoses and stratifies sepsis progression using biomarker levels. This paper reports a microfluidic biochip platform to detect proteins in undiluted human plasma samples. The device uses a differential enumeration platform that integrates Coulter counting principles, antigen specific capture chambers, and micro size bead based immunodetection to quantify cytokines. This microfluidic biochip was validated as a potential point of care technology by quantifying IL-6 from plasma samples (n = 29) with good correlation (R^2 = 0.81) and agreement (Bland–Altman) compared to controls. In combination with previous applications, this point of care platform can potentially detect cell and protein biomarkers simultaneously for sepsis stratification.

1. Introduction

Over the course of one-year, Intensive Care Units (ICU's) in the United States admit over 5 million patients. Annually, more than 1 million people are diagnosed with severe sepsis, costing the U.S. healthcare system approximately $24 billion.[1,2] Roughly 230 000 of these patients die, a mortality rate greater than the combined deaths from prostate cancer, breast cancer, and AIDS.[3] One major factor in these mortality rates is the inability to, accurately and quickly, diagnose potentially septic patients.

Clinics currently use the systemic inflammatory response syndrome (SIRS) criteria as a screening tool for the pro-inflammatory stage of sepsis. This tool is very non-specific and often results in very high false positive rates. For patients with SIRS positive criteria, the final diagnostic marker is a blood culture that may take 1–3 day for results. However, for septic patients, every hour delayed of proper antimicrobial medication can decrease 72 hour survival rates by roughly 7.6% per hour.[4] Current protocols for sepsis diagnosis and treatment are not frequent or specific enough to aid a physician's prognosis for different stages of sepsis. Moreover, the ideal treatment for each stage of sepsis (pro-inflammatory and anti-inflammatory) can be drastically different.[5,6]

Technologies capable of stratifying sepsis progression using biomarker levels are lacking. The use of biomarkers for the continuous monitoring of disease progression and patient response to treatment could help reduce high sepsis mortality rates. A hyper-inflammatory response is one of the first signs of development of sepsis; thus, a rapid, point of care device is needed to detect the acute immune response in patients suspected of sepsis.

Currently, lactate is the most common biomarker used to identify sepsis. However, although it is commonly assumed that lactate levels rise in patients with sepsis because decreased tissue perfusion of oxygen produces anearobic energy production, there are other explanations for the lactate elevations seen in sepsis.[7] Quantifying other biomarkers may help to enhance sepsis protocols by stratifying phases and continually guiding proper treatment. Potential sepsis biomarkers

[a] *Department of Bioengineering, University of Illinois at Urbana-Champaign, 1270 Digital Computer Laboratory, 1304 W. Springfield Ave., Urbana, Illinois 61801, USA. E-mail: rbashir@illinois.edu*
[b] *Micro and Nanotechnology Lab, University of Illinois at Urbana-Champaign, 208 N. Wright St., Urbana, Illinois 61801, USA*
[c] *Biomedical Research Center, Carle Foundation Hospital, 509 W University Ave., Urbana, Illinois 61801, USA*
[d] *Carle Illinois College of Medicine, 807 South Wright St., Urbana, Illinois 61801, USA*

† Electronic supplementary information (ESI) available. See DOI: 10.1039/c8lc00033f

‡ Michael Rappleye is now at: Department of Bioengineering, University of Washington, 3720 15th Ave NE, Seattle, WA 98105, USA.

have been correlated to key pathological responses, including organ dysfunction, (IL-6 and PCT), the hyper-inflammatory phase (IL-6, CRP, PMNs), and the immunosuppressive phase (monocyte HLA-DR).[7] Likewise, the relevance of the expression of cell surface markers such as CD64 and CD11b has been also linked to progression of sepsis.[7,8] In particular, several studies suggest IL-6 as a promising biomarker for providing early identification and prognostic information for monitoring septic patients.[9,10] In patients with bacterial sepsis, IL-6 levels start to increase 4 hours after the onset of systemic infection and normally peak between 8 and 24 hours. Thus, IL-6 serum levels are often elevated before the onset of SIRS symptoms and blood culture analysis.[9]

Healthy adults without inflammation have low IL-6 concentrations (<8 pg mL^{-1})[11] compared to septic episodes where the levels of this cytokine can dramatically increase. For instance, median IL-6 values of 1620 pg mL^{-1} were reported in early-onset neonatal sepsis.[12] Also, IL-6 concentrations exceeding >3000 pg mL^{-1} were reported when analyzing intensive care unit patients (adults, females and males).[9] Likewise, after analyzing the IL-6 levels in 56 patients, Harbarth *et al.* reported IL-6 concentrations >1000 pg mL^{-1} as the most discriminative parameter to predict sepsis-related death in infected patients at the time of admission.[13] In the same study, the IL-6 median values for septic shock, severe sepsis, and sepsis, were approximately 3000, 600, and 150 pg mL^{-1} respectively. In a study performed by Jekarl *et al.*,[10] IL-6 concentrations were analyzed in patients diagnosed with sepsis, and with severe sepsis/septic shock. In the case of survivors, the total mean values of IL-6 was 305 pg mL^{-1}, while in the case of non-survivors it was 1018 pg mL^{-1}.

Using cell and protein quantification, our research focuses on the clinical translation of this POC platform technology to diagnose and stratify sepsis. Our approach is based on a microfluidic differential counter technology that combines electrical coulter counting and immunocapture. We have successfully applied this approach to selectively enumerate leukocytes and quantify CD4/CD8,[14–16] as well as to quantify CD64 expression levels on neutrophils from 10 μL of whole blood.[17] In these previous contributions, cells were flowed through an aperture that has a current passing through it; the cell then blocked the current and causes a "spike" in signal. The number of spikes correlates to the number of cells traveling through the pore (entrance counter). Subsequently, the cells arrived at the capture chamber functionalized with target specific antibodies. Finally, the non-captured cells were counted again in the exit counter. Thus, by obtaining a total cell count at the beginning and a final count after capture, we were able to quantify the number of target cells in the sample.

In this paper, we adapted the same biochip platform to directly quantify proteins such as Interleukin 6 (IL-6) in undiluted human plasma samples. A key factor in the successful implementation of microfluidic coulter counting is the aspect ratio between the size of the cells (in the μm scale) and the dimensions of the aperture. When a cell passes through the aperture, it replaces a large percentage of conducting volume of with a resistive cell structure, producing a dramatic change in the impedance across the aperture (*i.e.* conductivity of the medium). To use similar channel dimensions but to able to detect nanometer size proteins, we developed a sandwich immunoassay for the detection of IL-6 on the surface of latex beads. Keeping similar aperture dimensions can also allow the potential to detect both cells and proteins simultaneously.

Although other contributions have reported the use of the electrical counting technology for the detection of proteins[18] and IgG,[19] this is first time, to the best of our knowledge, that the differential counting technology is reported for the detection of IL-6. In addition, our system includes some additional improvements, such as the use of pillars in the capture chamber (to increase the capture efficiency), that have not been reported before for the detection of proteins.

While this work uses IL-6 as a proof of concept target, the microfluidic biochip platform was designed to detect any protein by developing the sandwich immunoassay with appropriate target antibodies. Our future goal is to develop a single multi-marker POC device capable of simultaneous cell and protein detection from whole blood clinical samples. A fingerprinting of the pathological immune response through all stages of sepsis could define and diagnose sepsis, deter or prevent disease progression, while guiding treatment to save lives.

2. Experimental

2.1. Instrumentation

The flow of the required reagents for the capture chamber functionalization and the flow of sample through the biochip were performed using a Harvard PHD ULTRA™ pump (Harvard Apparatus, MA, USA). Electrical measurements were made combining a HF2LI Lock-in amplifier and a HF2CA Current amplifier, both from Zurich Instruments (Switzerland). The data acquisition was performed using LabVIEW 2013 (National Instruments, USA). The collected data was analyzed using MATLAB (MathWorks, USA).

Fluorescence was read on a Guava® easyCyte plus flow cytometer (EMD Millipore, USA). Absorbances were read on a Synergy HT (Biotek Instruments Inc., USA). The competitive curves were analyzed using a four-parameter logistic equation by means of GraphPad Prism 5 for Windows (GraphPad Software Inc., San Diego, CA, USA).

The shear stress in the capture chamber was simulated by using COMSOL Multiphysics 5.3.

2.2. Chemicals and reagents

The SU8-50 and SU-8 developer were purchased from Micro-Chem (MA, USA). Poly(dimethylsiloxane) (PDMS) prepolymer (Sylgard 184) and a curing agent were purchased from Dow Corning (MI, USA). The Pyrex wafers were purchased from University wafers (MA, USA).

Streptavidin from streptomyces avidinii (Cat# S4762), Bovine Serum Albumin (Cat# A3059) and Glycine (Cat# G8898-500G) were purchased from Sigma-Aldrich. CML Latex Beads 4% w/v, 7 μm (Cat# C37257); 2-(*N*-morpholino)ethansulfonic acid (MES) (Cat# 28390B; EDC (Cat# 22980); Sulfo-NHS (Cat# 21326); human IL-6 was purchased Shenandoah (Cat# 100-10). Human IL-6 Mab, clone: 5IL6 (Cat# M620); IL-6 Monoclonal Antibody (7IL6), Biotin (Cat# M621B); and R-phycoerythrin conjugate (SAPE) (Cat# S866) were purchased from Thermo Fisher Scientific. The Bradford solution (BIO-RAD protein assay cat No. 500-0006) was purchased from BIO-RAD laboratories GmbH (Munich, Germany).

Human Magnetic Luminex Screening Assay was purchased from R&D Systems. Human IL6/Interleukin 6 ELISA Kit (Sandwich Elisa) (Cat# LS-F9982) was purchased from LifeSpan Biosciences, Inc.

2.3. Buffers and solutions

PBS was 0.01 M phosphate buffer, 0.8%(w/v) saline solution and the pH was 7.5. MES was 0.1 M 2-(*N*-morpholino)ethansulfonic acid (pH 6).

2.4. Human plasma samples

Blood samples from patients suspected of sepsis (IRB number: 15094) were supplied by Carle Foundation Hospital (Urbana, IL. USA). The received samples were obtained from discards of already performed blood test from patients at Carle Hospital. The recruitment criteria were SIRS positive and/or blood culture ordered. From these samples, plasma was separated after centrifugation (1000*g*, 1 min, 4 °C) in our laboratories. The obtained plasma was stored at −80 °C until used.

In addition, pooled normal human plasma was obtained from Innovative Research (USA). The plasma aliquots (198 μL) were stored at −20 °C until used. The native concentration of IL-6 in the plasma was calculated <7 pg mL^{-1} by using the IL-6 ELISA Kit. The plasma samples were spiked by adding 2 μL of IL-6 to 198 μL of undiluted plasma.

2.5. Microfluidic structures

Microfluidic structures were fabricated for channels on the top of the electrodes and capture chambers. The master mold (negative) of these microfluidics devices was created by a standard SU8-photolithography process using SU8-50 negative photoresist on a Si wafer. The surface of the mold was silanized by 3-mercaptopropyltrimethoxysilane. The actual microfluidic structures were made from PDMS, in which elastomer is mixed with curing agent at the ratio of 10 : 1 with subsequent pouring on the master mold. After removing all bubbles using desiccator, it was cured at 90 °C for 60 min.

The capture chamber was a PDMS based device containing symmetrically distributed pillars. The dimensions of the capture chamber were 1.8 mm × 7.8 mm × 60 μm. The pillars were 60 μm tall and 40 μm in diameter, with 17 μm spacing between consecutives pillars. The subsequent pillar rows

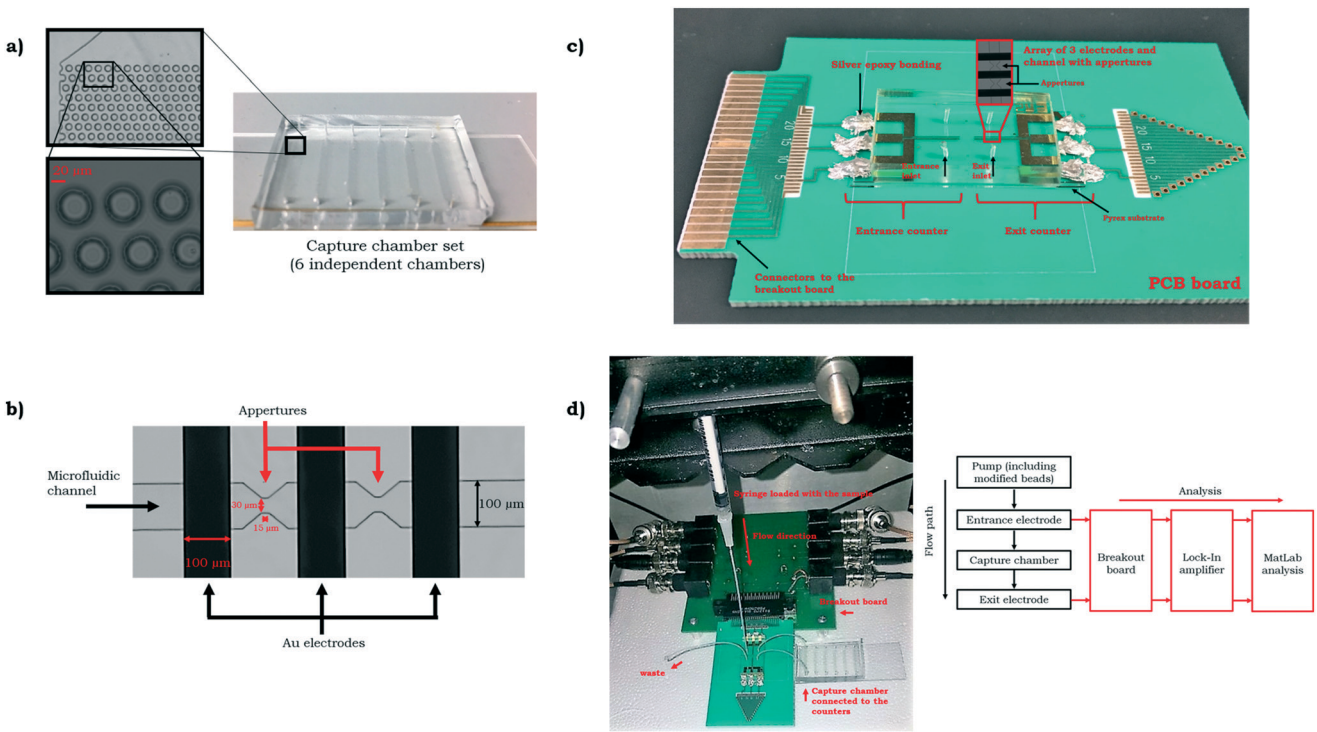

Fig. 1 Device components: a) the PDMS capture chambers were fabricated in sets of 6 independent chambers. The zoom-in optical images show top views of the pillars; b) detailed optical image (top view) of the microfluidic channel aligned over the electrodes. The volume of the microfluidic channel was reduced in the space between the electrodes (aperture); c) detailed optical image of the PCB board used for the electrical measurements; d) detailed optical image and schematic of the set-up used for the electrical measurements and analysis.

were staggered with a ratio 0.33. The total number of pillars per chamber is 8060 (total capacity = 1 μL). The capture chambers were fabricated in sets of 6 independent chambers (Fig. 1a).

2.6. Fabrication of the counter electrodes

Microfabricated co-planar gold electrodes were fabricated for the electrical counting. Thin Au/Ti (~127.5 nm thickness) electrodes (100 μm wide, 150 μm gap) were patterned on Pyrex wafers. For device design purposes, the wafers were diced grouping 2 arrays of 3 electrodes each, to function as entrance and exit counter.

The Pyrex substrate was first cleaned using absolute ethanol. Next, the Pyrex wafer was patterned using SPR220 and AP8000 photoresists to make a negative pattern of the electrodes. AZ400K developer is used to develop the wafer. Metal was deposited by sputtering and a standard lift-off process resolved the electrodes. The titanium layer (12.5 nm) was deposited prior the gold (115 nm) to improve adhesion to the Pyrex substrate.

A PDMS structure, including two independent microfluidic channels, was bonded on the top of the electrodes using APTES/GPTMS chemistry.[20] The bonding took place between the wafer and the PDMS structure. The dimensions of the channel (100 × 100 μm^2) were reduced in the space between the electrodes (15 × 30 × 15 μm^3). This portion of the channel was called the aperture. Fig. 1b shows an optical image (top view) of the microfluidic channel aligned over the electrodes. Every set of electrodes was connected to a PCB board by using silver conductive epoxy. An optical image of the counter electrodes (including the PCB board) can be seen in Fig. 1c.

The PCB board, together with another homemade breakout board (Wheatstone bridge circuit), serves as interface with the Lock-In amplifier.

2.7. Functionalization of the capture chambers

Functionalization took place in two steps to modify the capture chambers. First, the chambers were modified with streptavidin (used as universal capture agent). Second, BSA was used as blocking agent to minimize non-specific beads capture, eliminating possible available binding sites.

Thus, all the chambers in a set were serially connected to the pump. The pump was first loaded with 70% ethanol. The ethanol was flown through the chambers (50 μL min^{-1}) in order to completely remove the air from the chambers. Subsequently, PBS was flow through the chambers (50 μL min^{-1}) in order to completely remove the air from the chambers. Then, the pump was loaded with streptavidin (150 μL, 200 μg mL^{-1}). The streptavidin was infused through the set of chambers (35 μL, 15 μL min^{-1}), and then incubated at room temperature (30 min). This process was repeated twice. After the streptavidin incubation, the pump was loaded with BSA (1% w/v in PBS). The BSA was infused through the set of chambers (250 μL, 25 μL min^{-1}), and then incubated at room temperature (60 min). Finally, PBS was flown to wash out the unbonded reagents. The entire capture chamber functionalization process took 140 min. During this time, we were able to functionalize tens of chambers simultaneously.

2.8. Biofunctionalization of the particles

The carboxyl latex beads (7 μm) were covalently coupled to Ab_1IL-6 using slightly modified carbodiimide chemistry.[21] Briefly, the stored latex bead suspension (6 μL) was diluted with MES buffer (0.5 mL) and centrifuged (15 000*g*, 8 min, 4 °C). Then, the MES buffer was removed. The dry latex beads were suspended in a solution of 1 mM EDC and 0.5 mM Sulfo-NHS in MES buffer (0.1 mL) and mixed on a vortex (750 rpm, 15 min) to activate the carboxylic groups. Subsequently, the suspension was centrifuged (15 000*g*, 8 min, 4 °C), and the supernatant was separated to remove the excess reagents. The activated microparticles were resuspended again in a solution of Ab_1IL-6 (0.15 mL, 0.6 mg mL^{-1}) in PBS, and the suspension was shaken on a vortex (2 h, 750 RPM) to allow covalent homogenous coupling of the antibodies to the latex beads. Then, the whole mixture was centrifuged and washed with PBS (3 times, the supernatants were collected) to remove the unbound fraction. Subsequently, a solution of glycine (0.1 mL, 7.5 mg mL^{-1}) was added and the mixture shaken on a vortex (750 rpm) for 1 h to block the remaining activated carboxylic acid groups. Afterwards, the whole mixture was centrifuged and washed with PBS (1 time) to remove the unbound fraction. The supernatants collected after the Ab conjugation were used to evaluate the efficiency of the coupling strategy quantifying the antibody concentration in the supernatant and comparing with the concentration before the conjugation by the Bradford test.[22] The calculated bioconjugation efficiency was 71 ± 4%. Finally, the biohybrid microparticles (beads-Ab_1IL-6) were resuspended in PBS (0.1 mL), in order to obtain a final concentration of 640 μg mL^{-1} and 10 697 ± 181 beads-Ab_1IL-6 μL^{-1} (in terms of Ab_1IL-6 and modified-beads respectively) and stored at 4 °C until use. Typically, under these conditions, the modified latex beads were stable for about 2 months. The entire bead functionalization process, including the washing steps, took about 4 h.

2.9. Biochip measurement procedure

The entire biochip measurement procedure included: 1) the development of a sandwich immunoassay (performed on the latex beads) to specifically detect IL-6 (this process includes the incubation of the beads in plasma samples to capture target proteins); 2) the electrical counting, capture, and counting, which is all perform on-chip; and 3) the counting analysis and processing, which requires the analysis of the pulses produced by the modified-beads. The entire procedure is summarized in Fig. 2.

2.9.1. Sandwich immunoassay: off-chip procedure. The protein capture step was performed in 1.7 mL posi-click microcentrifuge Denville Scientific tubes, and all the

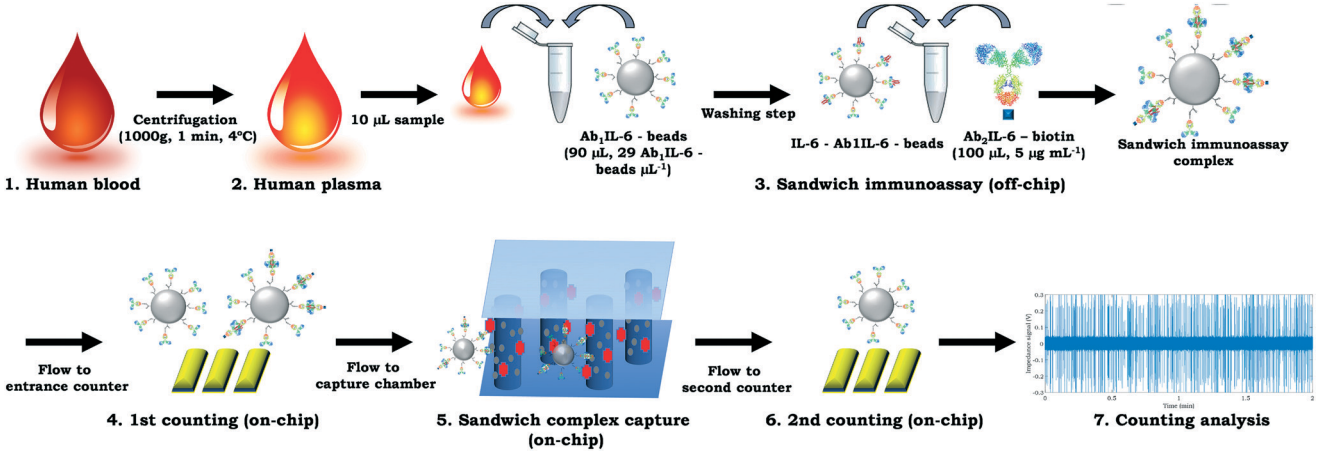

Fig. 2 Biochip measurement procedure. Off-chip procedure: first, plasma was separated from blood after centrifugation. Then, the plasma sample (containing the IL-6) was incubated with a solution of beads-Ab_1IL-6 (previously conjugated). After washing steps, a suspension of Ab_2IL-6-biotin was also incubated to obtain the sandwich immunoassay complex. On-chip procedure: first, the modified-beads were flowed through the entrance counter. Then, the beads with IL-6 (and as consequence with biotin) were specifically captured in the streptavidin + BSA-blocked capture chamber. Subsequently, the beads with no IL-6 (and as consequence with no biotin) were flowed through the exit counter. Finally, the counting analysis was performed, and the IL-6 concentration quantified.

quantities referred in this protocol are the amounts added per tube. After each incubation or washing step, the latex beads were separated from the supernatant on the sidewall by placing the tubes in a centrifuge (15 000*g*, 8 min, 4 °C).

A solution of beads-Ab_1IL-6 (29 beads-Ab_1IL-6 μL^{-1} in terms of latex beads, in PBS (1% BSA w/v), 90 μL, ~2616 beads-Ab_1-IL-6) was placed in the microcentrifuge tubes followed by the plasma samples (10 μL) or the IL-6 standard solutions (0–10^6 pg mL^{-1} in pooled normal human plasma or PBS, 10 μL) and incubated for 2 h at RT (950 RPM). Then, a suspension of Ab_2-IL-6-biotin (5 μg mL^{-1} in PBS (1% BSA w/v), 0.1 mL) was added to each tube and incubated for 30 min at RT (950 RPM). Subsequently, the obtained sandwich was washed with PBS (1% BSA w/v, 0.2 mL) and the modified latex beads resuspended in PBS (0.15 mL). The final solution, containing the modified-beads (beads-Ab_1IL-6 and beads-Ab_1IL-6-IL-6-Ab_2IL-6-biotin, ~17 modified-beads μL^{-1}), was analyzed by impedimetric techniques to quantify the IL-6 concentration in the sample as described below. The entire immunoassay process, including the washing steps, took about 3.5 h.

2.9.2. Electrical counting: on-chip procedure. First, the PCB board (containing the entrance and exit counters) was connected to the breakout board, in order to connect the counters to the Lock-In amplifier. Second, a syringe (loaded with the sample prepared as indicated in section 2.9.1.), as well as the streptavidin + BSA-blocked capture chamber, were serially connected to the counters, completing the whole biochip. The sample was flown at 20 μL min^{-1}. The entire set-up described (optical image and schematic) can be seen in Fig. 1d.

The three electrodes of every counter were connected to the Lock-In amplifier by the PCB boards connectors. Frequency interrogation of the modified-beads was performed at 303 KHz with up to a 5 V amplitude modulation voltage (applied to the middle counting electrode). When the voltage pulses start appearing for both counters, the data recording starts (up to 5 min) by using LabView at a sampling rate of 250 KHz. See ESI† for justification of chosen sampling rate.

2.9.3. Electrical counting analysis and processing. The data acquired from every experiment was analyzed in a customized MatLab code. The raw data was digitally filtered by the MatLab code as follows. The low-frequency noise including the baseline drifts were removed using the high-pass filter with a 20 Hz cut-off frequency. Power line interference of 60 Hz and its first harmonic (120 Hz) are removed by using two band stop filters with cutoff frequencies of (58, 62) Hz and (118, 122) Hz, respectively. The input frequency noise of 303 KHz was removed by using a low-pass filter with 303 KHz as a cutoff frequency.

The baseline noise was calculated as the average of the maximum amplitudes of all the voltage pulses measured. The contribution of the beads pulses to the average of the maximum amplitudes was negligible, as these pulses represents less than 1% of the entire entrance or exit data. The MatLab code counted the pulses when the amplitude of those pulses was 8 times the average of the baseline noise. This multiplying factor was found to clearly distinguish the beads-based pulses from electrical noise.

The figure of merit selected for the analysis was the percentage of capture:

$$\%\ \text{of capture} = \frac{\text{Entrance count} - \text{Exit count}}{\text{Entrance count}} \times 100$$

Standard calibration curve was constructed using GraphPad Prism 5 by plotting the percentage of capture data with respect to the IL-6 concentration and fitting the points to a four-parameter equation:

$$Y = \frac{(A-B)}{1+\left(\frac{x}{C}\right)^{D}} + B$$

where A is the maximum percentage of capture corresponding to the maximum IL-6 concentration, B is the minimum percentage of capture corresponding to the minimum IL-6 concentration, C is the concentration producing 50% of the maximal percentage of capture, and D is the slope at the inflection point of the sigmoid curve. The unknown IL-6 concentrations in the measured samples were calculated interpolating the respective percentage of capture in the standard calibration curve obtained.

The limit of detection (LOD) was calculated to be the concentration when the average response from percentage of capture in a negative control blank experiment (no IL-6) plus 3 times the standard deviation from that blank measurement.

3. Results and discussion

3.1. Assessment of the bioactivity of the biohybrid particles

The biofunctionality of the homogenous biohybrid particles (Ab_1IL-6-beads) was initially assessed using the sandwich immunoassay described in section 2.9.1. and using flow cytometry. Thus, the sandwich immunoassay was conducted as described in the experimental section, but with the final addition of a SAPE molecule to the sandwich immunoassay complex. After the incubation of the Ab_2-IL-6-biotin, the modified latex beads were washed and resuspended in a solution of SAPE (6.7 μg mL^{-1}, 150 μL), and incubated on a shaker for 30 min at RT in the dark. After the incubation step, the solution was transfer to a 96-well plate for the reading.

The developed immunoassay was assessed by interrogating solutions of IL-6 at distinct concentrations (0–10^6 pg mL^{-1}, 10 μL per tube in PBS or undiluted plasma) and measuring the SAPE fluorescence. The fluorescence was read in order to obtain the immunoassay response for each IL-6 concentration interrogated. As in the case of IL-6 described in section 2.9.1., the bioreagents were also diluted in PBS (1% BSA w/v). Thus, a calibration curve in PBS buffer was first obtained (Fig. 3a). The results indicated that the LOD of the sandwich immunoassay was 122 pg mL^{-1}, while the working range was from 10^2 to 10^6 pg mL^{-1}. The calibration curve is the result of two different experiments (n = 4 per IL-6 concentration).

Then, another calibration curve using undiluted plasma (instead of PBS) was also developed. Before spiking the plasma, the native IL-6 concentration was measured using an ELISA Kit to be <7 pg mL^{-1}. As it can be seen in the flow cytometry analysis in Fig. 3, the results of detecting IL-6 using PBS or undiluted plasma were very comparable, and the difference being less than 1%. The reason for this high similarity could be the 10-fold increase in volume during the first incubation step, which eliminates any matrix effects.

3.2. Principle of electrical differential counting

The microfluidic biochip developed was designed to count individual micron sized beads based on the Coulter counting principle. In the system, a microfluidic channel with a coulter aperture was aligned in between electrodes. When applying a potential between the electrodes (and across the aperture), the passage of a bead through the channel perturbs the electrical current within the aperture, creating a distinct impedance pulse. Thus, by selecting the appropriate threshold, the number of the pulses correlates to the count of the modified-beads flowing across the electrodes. The efficiency of the counting has been previously demonstrated, comparing the biochip counts with the control flow cytometer counts.[16] A video showing a modified-bead flowing through the channel (electrodes and aperture) can be seen in the ESI.†

The height of the pulses depends on the bead size, whereas its width depends on its speed. After the immunochemical procedure, two types of modified-beads remain: 1) beads-Ab_1IL-6; and 2) beads-Ab_1IL-6-IL-6-Ab_2IL-6-biotin. Although the electrical system can clearly distinguish between different bead types in heterogeneous beads populations based on their size and morphology (see ESI†), the system cannot differentiate between the beads with and without the proteins. However, when the two types of modified-beads (beads-Ab_1IL-6; beads-Ab_1IL-6-IL-6-Ab_2IL-6-biotin) were flown through the capture chamber, only the beads including IL-6 (and therefore, biotin), were specifically captured by the streptavidin-functionalized posts in the capture chamber. The beads without IL-6 (and therefore, without biotin), were not captured and enumerated by exit counter. By substracting the number of events at the exit counter from the number of

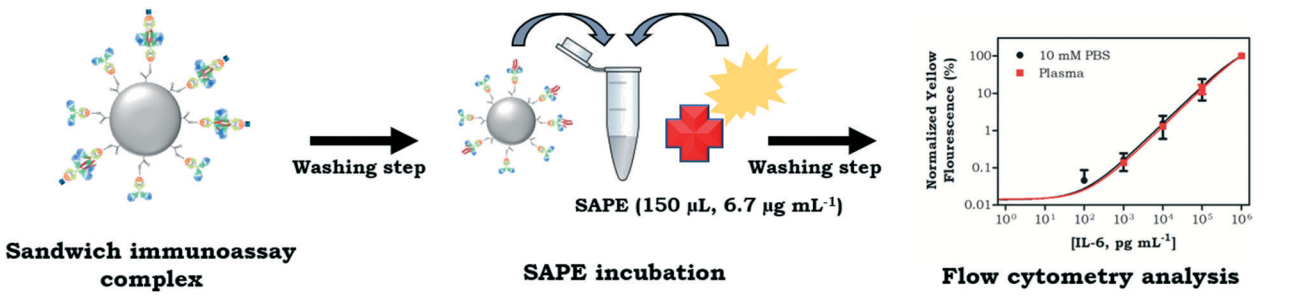

Fig. 3 Immunoassay assessment. The sandwich immunoassay was labeled with SAPE in order to assess the bioactivity of the biohybrid particles. The assay produced highly similar results when conducted in PBS *vs.* undiluted plasma.

event at the entrance, and dividing by the number of events at the entrance, the % of bead capture can be calculated (Fig. 4).

The two counters of the biochip are both configured to measure the relative impedance change caused by the passage of a modified-bead. (Fig. 4a).[17] The amplitude of a typical pulse produced by the beads was about 0.2–0.6 V. This amplitude, which depends on the bead size and the distance above the electrodes, was very similar to the values reported by Holmes *et al.* for impedimetric analysis of latex beads of similar size.[23] Also, the width of these pulses, which depends on the flow rate, was <2 ms (about 300 data points). These features allow a clear distinguish between the pulses and the baseline produce by the PBS buffer (Fig. 4b). The zoom-in figure shows the differential signal, which is a bipolar pulse for each passage of a modified-beads across the electrodes.

The use of pillars in the chamber significantly increased the capture surface area, therefore increasing the interactions between the biotinylated beads and the streptavidin (coated in the chamber). An optical image showing specific capture of modified-beads can be seen in Fig. 4c. The capture chamber was designed in order to: 1) maximize the bead-pillar interaction time; and 2) minimize the bead capture in the zero-velocity regions around the pillar. Thus, the subsequent pillar rows were staggered with a ratio 0.33. Applying this ratio, a more uniform bead-pillar can be ensured as it was previously demonstrated.[17] Inset figure (Fig. 4c) shows the results of the COMSOL simulation (heat bar scale units: Pa). It is well known that the shear stress is an important parameter affecting the capture of particles in a microfluidics channel.[24] In the simulation, blue color represents the regions where the shear stress was low, and as consequence, where the chance of capture was elevated. On the other hand, the gap between pillars from the same row (position: $\theta = \pm 90°$) is where the chance of capture was low. The results of the simulation were in good agreement with the capture results shown in Fig. 4c. Fig. 4d shows clearly the aspect ratio between one pillar and one captured bead.

Fig. 4e shows the histograms of representative counting using the entrance and exit counters. The comparison of the histograms shows that the counting in the entrance is higher than in the exit. This difference was expected as the modified-beads, including biotin, were counted in the entrance but not in the exit counter, as they were specifically captured in the chamber. The ratio between the counting in the entrance and in the exit, was used to quantify the concentration of IL-6. Thus, the figure of merit used was the percentage of

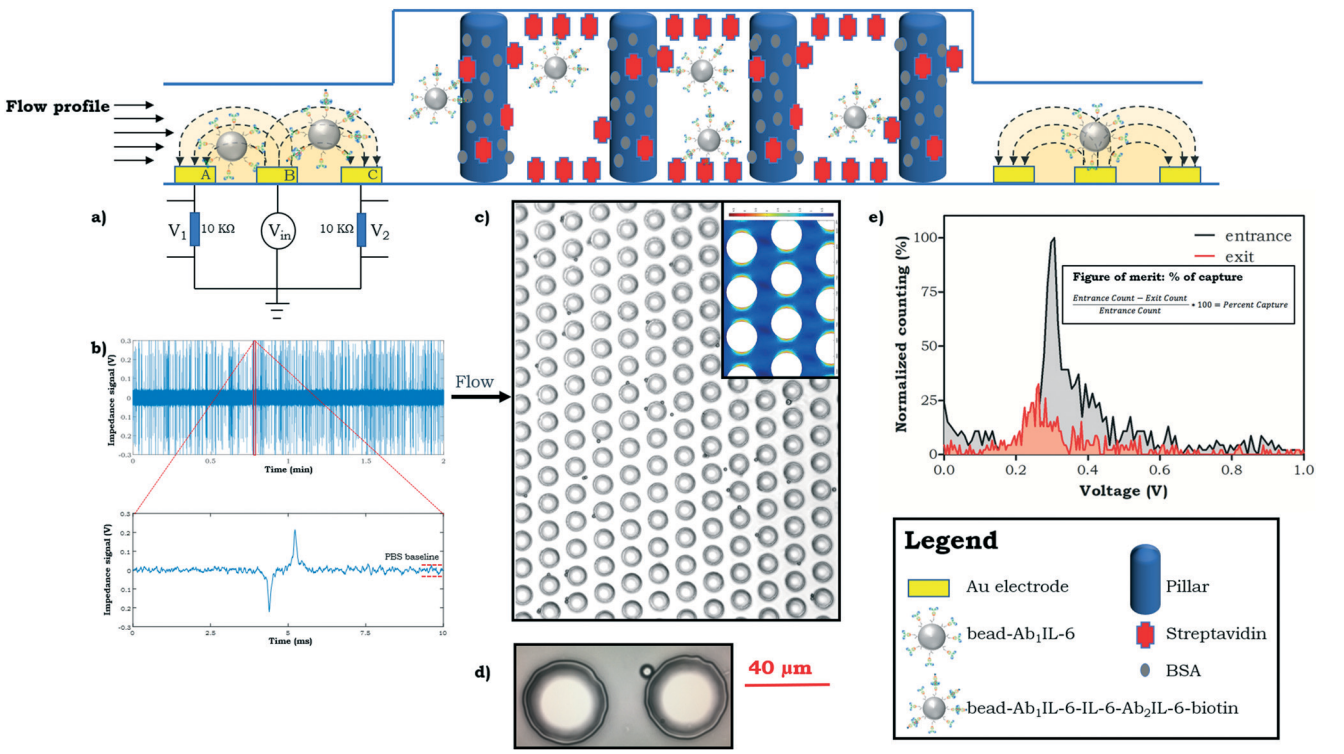

Fig. 4 Schematic of the principle of electrical differential counting of beads: a) the relative impedance was measured using the Wheatstone bridge circuit by acquiring output voltages across a 10 KΩ resistors; b) example of pulses produced by the modified-beads using the electrical counter. First plot shows pulses obtained during 2 min. Second plot shows a single pulse (scale: 0–10 ms); c) optical image of modified-beads specifically captured in the capture chamber. Inset: the shear stress simulation (units: Pa) shows where the options of streptavidin–biotin binding are higher (blue area, low shear stress); d) optical image showing the aspect ratio between one pillar and one captured bead; e) representative histograms of modified-beads counting comparing the capture in the entrance and exit counters. Inset: the % of capture is obtained by normalizing the differential count (inset).

capture (inset Fig. 4e). A video showing the specific capture of a biotinylated bead can be seen in the ESI.†

3.3. Critical bead diameter

The criteria for choosing the proper beads is not only based on the material (non-conductive) or functional groups (COOH), but especially on the particle size. From the hydrodynamic point of view, the bead diameter must be smaller than the gap between the pillars to prevent clogging.

Inglis *et al.*[25] developed a model that demonstrated that the critical particle size for fractionation depends on the micropost geometry, specifically on the gap between posts, the offset of posts in one row with respect to another, and whether the fluid is driven by hydrodynamics or by electroosmosis. We determined the diameter of the beads by solving the hydrodynamic equations presented by Inglis. As shown in Fig. 5a, the possible combinations of beads diameter/different pillar separations, solved by the model, were constrained by d_{max} and d_{min}. Thus, the model suggested that when having 17 μm of gap between the pillars, the beads diameter should be in the range of 7–14 μm. We chose 7 μm latex beads in order to also combine these beads with other beads and/or cells in the future with diameters in the range of 10 to 13 μm.

3.4. Effect of the BSA blocking step

After the streptavidin functionalization, the possible available binding sites were blocked with BSA (1% in PBS). The inclusion of BSA dramatically reduced the non-specific absorption as this can be seen in Fig. 5b. When BSA was not used as blocking agent (capture chamber only functionalized with streptavidin), the beads non-specific captured were about 60%. However, when using BSA, the non-specific absorption was below 10%.

3.5. Effect of the flow rate

The efficient and specific capture of beads require the optimization of not only the capture chamber design, but also the flow rate. The sample flow rate plays a very important role in the design of the device, as increasing the flow rate will reduce the time of the analysis but also result in different shear stress for the bead capture.[26] Fig. 5c shows the effect of the flow rate on the non-specific absorption, when using BSA as blocking agent. When the flow rate was low, for instance 5 or 10 μL min^{-1}, the obtained non-specific absorption was high, about 80% and 50% respectively. However, when working at 20 μL min^{-1}, the non-specific absorption was below 10%. Thus, a flow rate of 20 μL min^{-1} was selected. It is also remarkable that some of this 10% of non-specific absorption can be also attributed to losing some of the beads in the tubing connecting the counters with the capture chamber. However, the % of beads loosed because the tubing can be completely eliminated when having the electrical counters and the capture chamber in the same microfluidic device (not connected by tubing).

3.6. Detection of IL-6 with the microfluidic biochip

The ability of the microfluidic biochip to measure IL-6 was assessed by incubating for 2 h the standard solutions of IL-6 (0–10^6 pg mL^{-1}, in PBS) with the beads-Ab_1IL-6 solution, before adding the Ab_2IL-6-biotin suspension and then following the biochip measurement procedure described in section 2.9.2.

In these experiments, the percentage of capture was calculated to obtain the biochip response corresponding to each IL-6 concentration added. As the microfluidic biochip was able to count individual biologically modified micron sized bead, the % of capture was calculated by normalizing the subtraction of the number of events in the exit from the number of event in the entrance. As expected, the % of capture signal recorded was in this case proportional to the concentration of IL-6 in the buffer samples (Fig. 6a). Thus, when performing the measurements in PBS an EC50 value of 734.4 pg ± 0.2 pg mL^{-1}, a LOD of 127 pg mL^{-1}, and a working range up to 5135 pg mL^{-1} (calculated from the signal at 80% of the normalized calibration curve) were achieved.[9,10,12,13] The features of the IL-6 calibration curve are summarized in the table in Fig. 6a. If required, the LOD achieved can be easily improved by reducing the reaction volume. For instance, the 10 μL of samples could be conjugated with only 10 μL of the beads-Ab_1IL-6 solution, instead of 90 μL, but 9 times concentrated. By reducing the reaction volume, a shorter conjugation time is also expected.

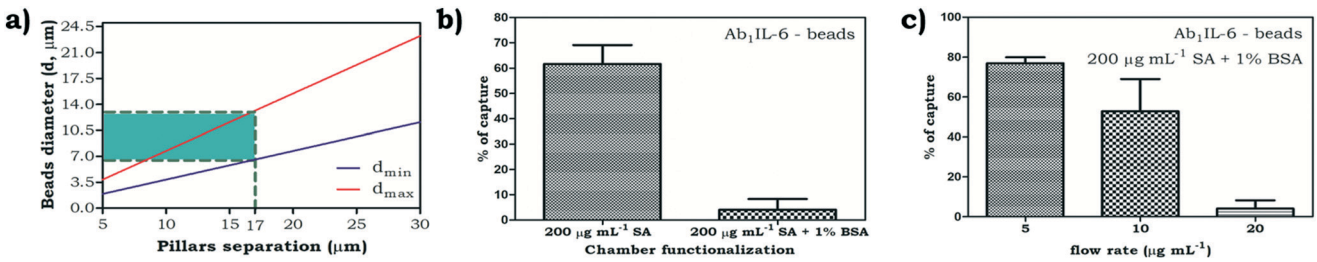

Fig. 5 Beads characterization: a) critical particle size. The simulation suggested that 7 to 14 μm beads could be used when the pillars separation is 17 μm; b) blocking effect (flow rate = 20 μL min^{-1}). When 1% BSA was using as blocking agent, the non-specific absorption was <10%; c) flow rate effect. Increasing the flow rate up to 20 μL min^{-1} reduced the non-specific absorption to values <10%.

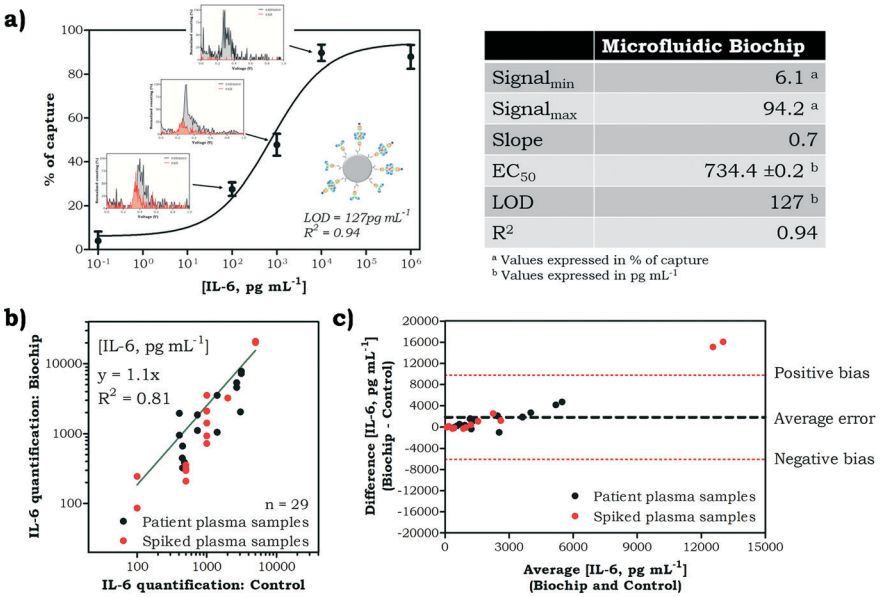

	Microfluidic Biochip
$Signal_{min}$	6.1 [a]
$Signal_{max}$	94.2 [a]
Slope	0.7
EC_{50}	734.4 ±0.2 [b]
LOD	127 [b]
R^2	0.94

[a] Values expressed in % of capture
[b] Values expressed in pg mL^{-1}

Fig. 6 IL-6 detection: a) calibration curve obtained using the electrical differential counting system. Inset: Representative histograms of different modified-beads counting along the working range of the calibration curve. Table: Features of the IL-6 calibration curve; b) comparison of the IL-6 quantification using the electrical differential counting method and controls; c) Bland–Altman analysis comparing the IL-6 concentrations obtained using the biochip and controls.

3.7. Detection of IL-6 with the microfluidic biochip in human plasma samples

As the studies performed in section 3.1 demonstrated, the developed immunoassay offered comparable results when detecting IL-6 from PBS or undiluted plasma samples. Based on this, the calibration curve obtained in Fig. 6a, was used to quantify the IL-6 concentrations in 29 human plasma samples. These plasma samples were obtained from: 1) potentially septic patient blood samples (15); and 2) spiked pooled normal human plasma (14).

The concentration of IL-6 in the patient samples was also analyzed using Luminex® and these results were using as control. The IL-6 concentration of the analyzed samples was in the range from 100 to 5000 pg mL^{-1}. The comparison between the biochip IL-6 quantification and the control can be seen in Fig. 6b. It is very encouraging to see that the IL-6 concentration in all the potentially septic patient samples analyzed was in the measurement range of our device. This was especially useful because no dilution of the samples was necessary.

A correlation coefficient R^2 = 0.81 (slope = 1.1) was obtained for the 29 analyzed samples, demonstrating a good linear correlation. In addition to the correlation, the agreement between the quantification performed and the controls was also tested using the Bland–Altman plot (Fig. 6c). As can be seen in the plot, most of the analyzed samples (27) are well in between the limits of agreement. The two samples that are out of the limits are the samples with high IL-6 concentrations. These concentrations are in the limit of the working range of the biochip developed. As consequence, in this case, the information provided by the biochip would be that the IL-6 concentrations are >5135 pg mL^{-1} (working range limit).

As previously mentioned, our group has demonstrated the electrical differential counting technology for cells.[15,17] Also Mok *et al.*[18] reported the detection of IL-6 from 50% human serum using an electrical counting system (non-differential). In this system the captured chamber used did not include pillars and the LOD obtained was 50 pM (1050 pg mL^{-1}, MW IL-6 = 21 KDa).

Other recent on-chip methods for detection of protein biomarkers, based on electrochemical[27] or optical[28] approaches, have been reported in the literature. However, to the best of our knowledge, none of those methods have demonstrated to be compatible with measurement of cells and proteins in the same platform.

The presented method is completely compatible with detection and capture of cells. Combining the detection of proteins and cells will be the focus of our next study.

4. Conclusions

A novel microfluidic biochip for the quantification of IL-6 has been developed and its performance in undiluted human plasma samples has been demonstrated. This biochip, based on the differential electrical counting technology and the use of capture chambers for the specific capture of bead complexes including IL-6, has demonstrated the electrical enumeration of modified-beads and the quantification of the cytokine.

The sandwich immunoassay, used for the specific detection of IL-6, was performed using about 2600 beads-Ab_1IL-6. Each measurement took 5 min and with a flow rate of about 6 modified-beads per s. The limit of detection achieved (127 pg mL^{-1}), was well below the IL-6 levels reported in septic

patients. Twenty-nine plasma samples analyzed for the system validation were obtained from potentially septic patient blood samples (15) and from spiked pooled normal human plasma samples (14).

Although several improvements are necessary to bring the current design to clinical translation as a complete POC device, the ability to selectively quantify a target protein biomarker using our platform is a fundamental stepping stone towards a multi-marker POC device for the combined detection of cells and proteins from whole blood clinical samples.

Author contributions

E. V. and R. B. designed the study. E. V. wrote and R. B., J. B, U. H., T. G., and K. W. edited the manuscript. E. V., U. H., and T. G. designed the devices. E. V., J. B., J. L., M. R., J. W., R. H., N. M., A. H., and C. L. performed the experiments. U. H., E. V. R. H., and J. L. worked in the MatLab code. T. G. worked in the COMSOL simulations and equations analysis. Z. P. run the Luminex® assays. D. A., Z. H., N-T. H., and N. M. fabricated the devices. K. W. performed clinical patient adjudication.

Conflicts of interest

Rashid Bashir and Umer Hassan declare competing financial interests in Prenosis, Inc. working to commercialize technologies for detection of cells and proteins.

Acknowledgements

The authors thank E. Iniguez, V. Reddi, J. Eardley and R. Grubbs from Carle Foundation Hospital for their help in conducting this study. The authors also thank M. Saadah, A. Carlson, A. Larson, J. Lothridge, N. Mandhan, N. Nawar, K. Schultheis, J. Varghese, C. García, V. Font-Bartumeus, J. Tiao, S. Gargya, V. Kindratenko, C. Pollock-Muskin, H. Shapland, A. Summitt, Y. Yedetore for their help in experiments, devices fabrication, and samples manipulation. This work was supported by USDA ARS for funding support through the Center for Food Safety Engineering at Purdue University (project number 1935–42000-035), and funds from the University of Illinois at Urbana-Champaign.

References

1 D. F. Gaieski, J. M. Edwards, M. J. Kallan and B. G. Carr, *Crit. Care Med.*, 2013, **41**, 1167–1174.
2 T. Lagu, M. B. Rothberg, M.-S. Shieh, P. S. Pekow, J. S. Steingrub and P. K. Lindenauer, *Crit. Care Med.*, 2012, **40**, 754–761.
3 N. K. Adhikari, R. A. Fowler, S. Bhagwanjee and G. D. Rubenfeld, *Lancet*, 2010, **376**, 1339–1346.
4 A. Kumar, D. Roberts, K. E. Wood, B. Light, J. E. Parrillo, S. Sharma, R. Suppes, D. Feinstein, S. Zanotti, L. Taiberg, D. Gurka, A. Kumar and M. Cheang, *Crit. Care Med.*, 2006, **34**, 1589–1596.
5 O. Liesenfeld, L. Lehman, K.-P. Hunfeld and G. Kost, *Eur. J. Microbiol. Immunol.*, 2014, **4**, 1–25.
6 J. Cohen, J.-L. Vincent, N. K. J. Adhikari, F. R. Machado, D. C. Angus, T. Calandra, K. Jaton, S. Giulieri, J. Delaloye, S. Opal, K. Tracey, T. v. d. Poll and E. Pelfrene, *Lancet Infect. Dis.*, 2015, **15**, 581–614.
7 J. D. Faix, *Crit. Rev. Clin. Lab. Sci.*, 2013, **50**, 23–36.
8 C. Pierrakos and J.-L. Vincent, *Crit. Care*, 2010, **14**, R15.
9 J. C. Schefold, D. Hasper, S. v. Haehling, C. Meisel, P. Reinke and H.-G. Schlosser, *Clin. Biochem.*, 2008, **41**, 893–898.
10 D. W. Jekarl, S.-Y. Lee, J. Lee, Y.-J. Park, Y. Kim, J. H. Park, J. H. Wee and S. P. Choi, *Diagn. Microbiol. Infect. Dis.*, 2013, **75**, 342–347.
11 D. K. Thompson, K. M. Huffman, W. E. Kraus and V. B. Kraus, *PLoS One*, 2012, **7**, e30659.
12 H. Martin, B. Olander and M. Norman, *Pediatrics*, 2001, **108**, 1–6.
13 S. Harbarth, K. Holeckova, C. Froidevaux, D. Pittet, B. Ricou, G. E. Grau, L. Vadas, J. Pugin and G. S. Network, *Am. J. Respir. Crit. Care Med.*, 2001, **164**, 396–402.
14 N. N. Watkins, S. Sridhar, X. Cheng, G. D. Chen, M. Toner, W. Rodriguez and R. Bashir, *Lab Chip*, 2011, **11**, 1437–1447.
15 N. N. Watkins, U. Hassan, G. Damhorst, H. Ni, A. Vaid, W. Rodriguez and R. Bashir, *Sci. Transl. Med.*, 2013, **5**, 214ra170.
16 U. Hassan, N. N. Watkins, B. R. Jr, G. Damhorst and R. Bashir, *Nat. Protoc.*, 2016, **11**, 714–726.
17 U. Hassan, T. Ghonge, B. R. Jr., M. Patel, M. Rappleye, I. Taneja, A. Tanna, R. Healey, N. Mansury, Z. Price, T. Jensen, J. Berger, A. Hasnain, E. Flaugher, S. Liu, B. Davis, J. Kumar, K. White and R. Bashir, *Nat. Commun.*, 2017, **8**, 15949.
18 J. Mok, M. N. Mindrinos, R. W. Davis and M. Javanmard, *Proc. Natl. Acad. Sci. U. S. A.*, 2014, **111**, 2110–2115.
19 Z. Lin, X. Cao, P. Xie, M. Liu and M. Javanmard, *Biomed. Microdevices*, 2015, **17**, 119.
20 L. Tang and N. Y. Lee, *Lab Chip*, 2010, **10**, 1274–1280.
21 E. Valera, A. Muriano, I. Pividori, F. Sánchez-Baeza and M. P. Marco, *Biosens. Bioelectron.*, 2013, **43**, 211–217.
22 M. M. Bradford, *Anal. Biochem.*, 1976, **72**, 248–254.
23 D. Holmes, D. Pettigrew, C. H. Reccius, J. D. Gwyer, C. v. Berkel, J. Holloway, D. E. Davies and H. Morgan, *Lab Chip*, 2009, **9**, 2881–2889.
24 T. Ghonge, A. Ganguli, E. Valera, M. Saadah, G. L. Damhorst, J. Berger, G. P. Diaz, U. Hassan, M. Chheda, Z. Haidry, S. Liu, C. Hwu and R. Bashir, *APL Bioengineering*, 2017, **1**, 016103.
25 D. W. Inglis, J. A. Davis, R. H. Austin and J. C. Sturm, *Lab Chip*, 2006, **6**, 655–658.
26 U. Hassan and R. Bashir, *Lab Chip*, 2014, **14**, 4370–4381.
27 A. Baraket, M. Lee, N. Zine, M. Sigaud, J. Bausells and A. Errachid, *Biosens. Bioelectron.*, 2017, **93**, 170–175.
28 M. Anastasopoulou, A. Malainou, A. Salapatas, N. Chronis, I. Raptis and K. Misiakos, *Sens. Actuators, B*, 2018, **256**, 304–309.

